Available online at www.sciencedirect.com
SCIENCE DIRECT
Thermochimica Acta 445 (2006) 179–184
thermochimica acta
www.elsevier.com/locate/tca

DSC examination of the rotator cuff muscles in rabbits

I. Szabó [a,*], G. Bognár [a], I. Magda [b], R. Garamvölgyi [c], G. Czobel [d], L. Nőth [d], L. Kereskai [e], P. Bogner [f]

[a] Department of Orthopedic Surgery, Medical School, University of Pécs, H-7624 Pécs, Szigeti Str. 12, Hungary
[b] Department of Radiology, Medical School, University of Pécs, H-7624 Pécs, Szigeti Str. 12, Hungary
[c] Diagnostic and Oncoradiology Institute, University of Kaposvár, H-7400 Kaposvár, Guba Sándor Str. 40, Hungary
[d] Department of Traumatology, Medical School, University of Pécs, H-7624 Pécs, Szigeti Str. 12, Hungary
[e] Department of Pathology, Medical School, University of Pécs, H-7624 Pécs, Szigeti Str. 12, Hungary
[f] Institute of Laboratory Medicine, Medical School, University of Pécs, H-7624 Pécs, Szigeti Str. 12, Hungary

Available online 22 May 2006

Abstract

Rotator cuff tear is a common musculoskeletal disorder with pathological changes occurring in the structure of the rotator cuff musculature (fatty infiltration). Severe fatty infiltration, observed on MRI or CT scan, negatively influences the result of rotator cuff reconstruction in human beings. The basic histological and biochemical alterations in fatty infiltration of the rotator cuff muscle with torn tendon are still not clear. Differential scanning calorimetric (DSC) examination is a well-established method for the demonstration of thermal consequences of local and global conformational changes in biological systems. With foregoing studies, authors have demonstrated the feasibility of DSC in the investigation of the musculoskeletal system. The aim of this study was to establish the thermograms of the rotator cuff muscles with normal and torn tendons, experimentally induced in rabbits. The DSC results clearly proved that definitive differences are present between the muscles with normal and torn tendons, which have also been demonstrated by MRI and CT scans.

Keywords: Rotator cuff tear; CT; DSC; MRI

1. Introduction

The disorders of the rotator cuff and its muscles are the most common reasons of the shoulder dysfunction and pain. The cuff is a continuous tendinous band around the humeral head. It is built up of four tendons: supraspinatus, infraspinatus, subscapularis and teres minor. The functions of the rotator cuff and its muscles are, the active rotation, active elevation of the arm and it is a dynamic stabilizer of the humeral head in the glenohumeral joint. Rotator cuff tendon tear leads to fatty infiltration and atrophy of the muscle unit, depending on the magnitude of rupture and time elapsed from the injury [1–4]. Experimental and clinical data suggest the correlation between the outcome of rotator cuff repair and degree of fatty muscle degeneration [2,4–6]. Phoenix et al. has developed a method to record muscle mass and fat in human dystrophic muscle by MRI [7]. Goutallier et al. used a 5-stage CT scale for evaluation of supraspinatus muscle fatty degeneration [1]. Nakagaki et al. and Thomazeau et al. used MRI for the same purpose [2,3]. Fabis et al. analyzed the relationship between the rabbit supraspinatus muscle contractile properties and CT image of the muscle belly after detachment of its tendon from the greater tubercle [8,9]. The morphometric changes in the muscle with a detached tendon were also analyzed [10]. Fatty infiltration and atrophy of the rotator cuff muscles should be distinguished. Evidence of at least partial reversal of muscle atrophy but of absence of reversal of fat accumulation after successful tendon repair has been published [1,3,11–13]. So after solving the underlying problem of the atrophy, the muscle can regain its strength, which means that surgical intervention can be more successful. The atrophy can be caused by for example inactivation of the muscle due to pain or failure of its supplying nerve. These changes can alter the structure of muscle or they can influence the pathway of ATP hydrolysis.

Differential scanning calorimetric (DSC) is widely used to monitor the thermal denaturation of biological macromolecules, e.g. muscle proteins [14–18]. Most of these papers refer to the

* Corresponding author. Tel.: +36 72 536 206; fax: +36 72 536 210.
E-mail address: szaboi@hotmail.com (I. Szabó).

0040-6031/$ – see front matter © 2005 Elsevier B.V. All rights reserved.
doi:10.1016/j.tca.2005.10.011

protein solutions but only few labs are working on muscle fibres as supramolecular system [19–22]. Muscle contraction and other events of cell motility are based on the cyclic interaction of the head portion of myosin with actin during the myosin-catalysed ATP hydrolysis. In isolated form of myosin the half-life of this process is only several seconds at 25 °C, therefore further stabilisation is needed in muscle fibres to perform detailed structural or dynamic analysis of this transition state. It was found that a complex of myosin with ADP and orthovanadate formed a stable structure, which allowed the studies on the conformation in this intermediate [23,24]. To look into the details we simulated the long lasting intermediate states of ATP hydrolysis cycle, namely the rigor, the strong binding (AM·ADP state) and weak-binding (AM·ADP·P_i) states, where AM stands for actomyosin. Therefore, we analyzed the relationship between the rabbit supraspinatus and infraspinatus muscle thermal changes, the histological properties and the CT and MRI images of the muscle belly 6 month after detachment of its tendon or cut its supplying nerve. According to the literature DSC could be a suitable method for demonstration of thermal consequences of local as well as global conformational changes of the cross-striated muscle structure [25–27]. It is very characteristic for the actual functional and structural states of different muscles; it behaves as a fingerprint [19].

2. Materials and methods

2.1. Animals

The University Animal Care Committee approved the protocol for this study. We used 37 adult male Pannon Meat rabbits (mass: 3–4 kg) for this research. They were anesthetized with Primazin 2% injection (0.4 ml/kg) supplemented by skin infiltration with 1% xylocaine. The shoulder was exposed by a longitudinal anterolateral incision. The omovertebral and deltoid muscle were retracted. Depending on the goal of the procedure the suprascapular nerve or the supraspinatus and infraspinatus tendon were identified. Seven rabbits were used for a pilot study (group 0) of the rotator cuff and the suprascapular nerve anatomy, and for establishing the DSC and histological properties of the healthy rabbit cuff muscles. The remainder 30 rabbits were divided into two groups. In group A the supraspinatus and infraspinatus tendons were detached from the greater tuberosity to model fatty infiltration. In group B the supplying suprascapular nerve were cut to model denervation atrophy. The fasciae of the muscle and the skin were sutured in separate planes. Neither postoperative immobilization nor any restrictions in activity were used. The rabbits had access to water and food. Six month after the first procedure, a second intervention was performed to take histological samples and the animals were sent to euthanasia with an overdose of 1 ml T61 (made by Intervet: 0.2 g embutramide and 0.05 g mebenzonium–iodide in aqueous solution) injection.

2.2. Imaging techniques

Computed tomography scan (Siemens Somatom +4) and MRI (General Electric Ovation Sigma 0, 35T open MR) examinations were performed on all of the proper rabbit muscles before the two procedures for the evaluation of radiological changes during the follow-up period and for establish the presence, absence and degree of muscular changes. The fatty infiltration and muscle atrophy were evaluated by examination of axial CT scan sections obtained with soft tissue window and T2-weighted MRI sequences.

2.3. Histology

Muscle samples were taken from the supraspinatus muscle belly for the histological examinations and for the DSC measurements closely after the imaging. For the histological examination the specimens were fixed in 10% neutralized formalin for a week, decalcified with formic acid for 2 weeks, embedded in paraffin, and cut to a thickness of 5 μm. All sections were stained with hematoxylin–eosin. The histological morphometry was performed with Nikon Eclipse E400 light microscope (usual magnification 100) to examine the changes of the muscle structure.

2.4. DSC measurements

The specimens for the DSC measurement (in each experimental set three from one supraspinatus muscle) were prepared in 1:1 mixture of glycerol and mammal ringer (MR), fixed on a glass rod. They were many times washed in MR and MR + glycerol mixture to make the membrane system more penetrable (chemical skinning) for ADP and orthovanadate to be available to prepare the mimicked intermediate states of ATP hydrolysis.

Thermal unfolding of muscle proteins in different ATP hydrolysis intermediate states induced by rigor (R), R + ADP and R + ADP·V_i (V_i stands for orthovanadate to mimick the ADP·P_i state) was monitored by a SETARAM Micro DSC-II calorimeter. All experiments were conducted between 0 and 100 °C. The heating rate was 0.3 °K/min in all cases. Conventional Hastelloy batch vessels were used during the denaturation experiments with 850 μL sample volume (muscle fibres plus buffer) in average. Typical muscle wet weights for calorimetric experiments were between 200 and 250 mg. Rigor buffer was used as a reference sample. The sample and reference vessels were equilibrated with a precision of ±0.1 mg. There was no need to do any correction from the point of view of heat capacity between sample and reference vessels. The repeated scan of denatured sample was used as baseline reference, which was subtracted from the original DSC curve. Calorimetric enthalpy was calculated from the area under the heat absorption curve by using two-point setting SETARAM peak integration.

3. Results

3.1. CT and MRI results

The CT scan (Fig. 1a) and MRI (Fig. 1b) pictures of the control group (group 0) show symmetric and intact shoulder structure. In group A (tendon detached) CT scan (Fig. 2a) and MRI (Fig. 2b) revealed fatty degeneration of the supraspinatus

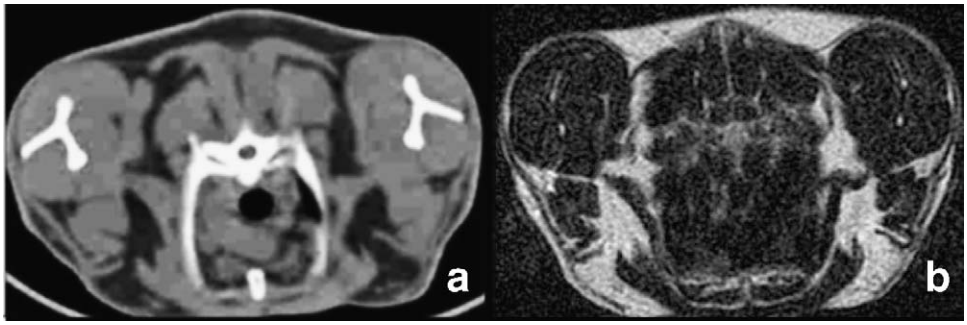

Fig. 1. CT scan (a) and MRI record (b) of the rabbit shoulder (saggital cross section) of intact (group 0).

Fig. 2. CT (a) scan of the rabbit shoulder (saggital cross section) 6 months after tendon detachment (group A). Fatty infiltration can be revealed in the supraspinatus muscle. MRI picture (b) from the same area with identical result.

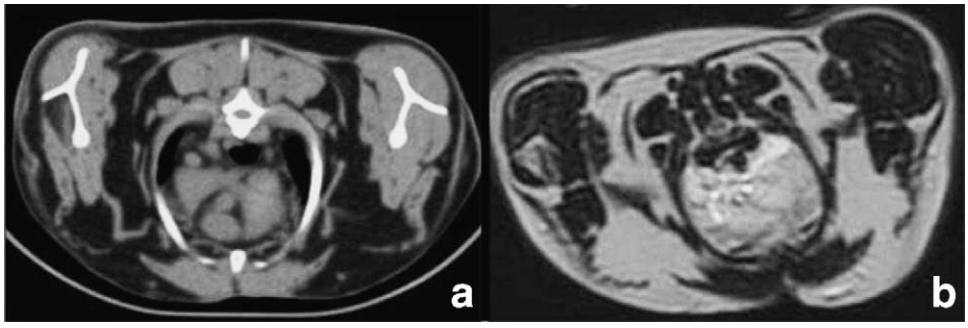

Fig. 3. CT (a) scan of the rabbit shoulder (saggital cross section) 6 months after nerve cut (group B). Atrophy of the suprapinatus, infraspinatus muscles can be revealed, but fatty infiltration cannot be observed. The diameter decreased of the both muscles, and the fat accumulated around the muscle belly. The result is the same in MRI photo (b) too.

muscle of the side operated on, which confirm the effect of the tendon detachment on the fatty infiltration of the rotator cuff muscles. In group B (nerve cut) CT scan (Fig. 3a) and MRI (Fig. 3b) showed the atrophy of the supraspinatus, infraspinatus muscles, but fatty infiltration cannot be observed. The diameter decreased of the both muscles, and the fat accumulated around the muscle belly.

3.2. Histological results

The histological examinations confirmed the CT and MRI findings. The first section was taken from the intact supraspinatus muscle belly (Fig. 4a). In group A (tendon detached) the section showed the reductions in diameter of the muscle fibres. Focal necrosis of single muscle fibers with inflammatory infiltration, mostly by phagocytes, was seen. The endomysial and perimysial connective tissue and fat tissue between the muscle fibres were increased. The interstitial volume was greater than in group 0. This is typical for fatty infiltration (Fig. 4b) By group B (nerve cut) histology revealed decreasing number of the muscle fibres, and increasing mass of the connective tissue between the muscle fibres (Fig. 4c) In this stage fat accumulated around the muscle belly, whereas by fatty infiltration fat appears in the structure of the muscle too.

3.3. DSC results

The thermal denaturation in each muscle set and ATP hydrolysis state showed a complex unfolding process characterising at least three or four discrete molecular regions with different thermal stabilities (Figs. 5–7). The DSC scan of *intact healthy muscle* as reference showed an unfolding in rigor at 52.2, 59.2

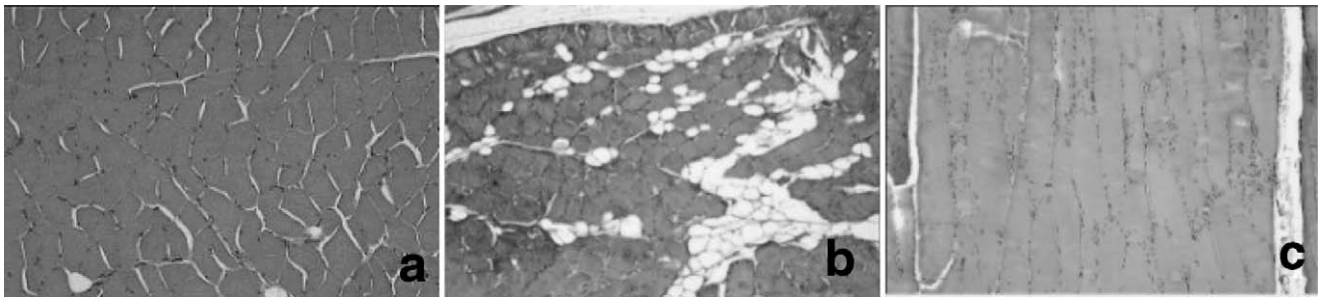

Fig. 4. Histology of intact (group 0) supraspinatus (a), 6 months after tenotomy (group A) an increase in endomysial and perimysial connective tissue as well as fat tissue can be observed (b) and 6 months after nerve cut (group B) a decrease in number of the muscle fibres, increase in endomysial and perimysial connective tissue, but fatty infiltration cannot be observed (c) (HE, ×250). All sections were stained with hematoxylin–eosin. Nikon Eclipse E400 light microscope was used (with a usual magnification of 100).

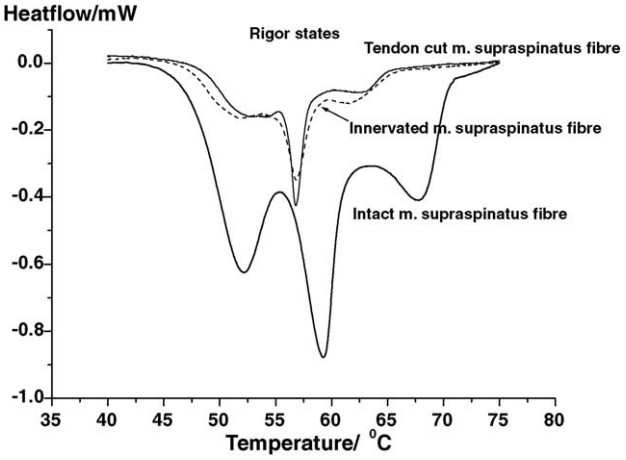

Fig. 5. DSC scan of rigor state (intact: thicker solid line, tendon cut: solid line and innervated with dotted line. Endotherm effect in downward direction.).

and 67.8 °C. These values were 53.5, 56.8 and 61.6 °C for *tendon detached* as well as 52, 56.8 and 62.6 °C for *denervated muscles* indicating the thermal consequences of structural changes (Fig. 5).

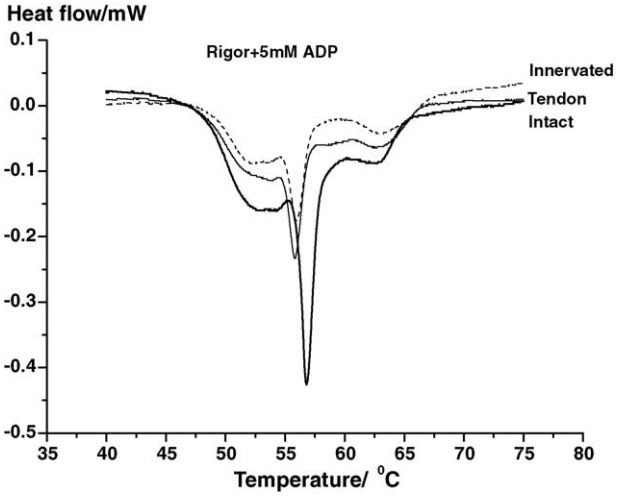

Fig. 6. Thermal denaturation curves of strong binding (R + ADP) state. Symbols are the same as in Fig. 1.

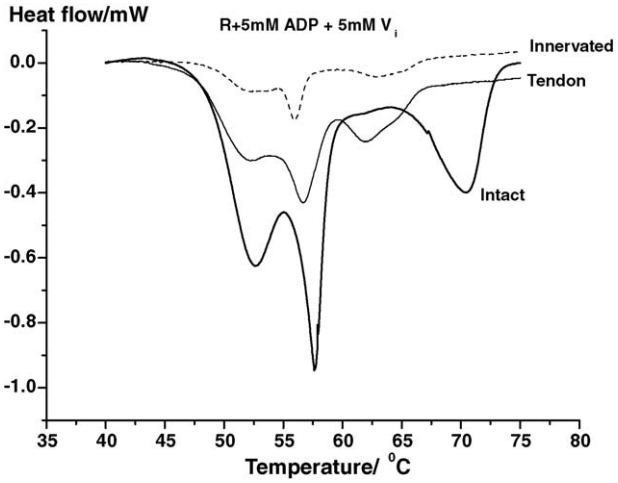

Fig. 7. Thermal unfolding of weak-binding state (R + ADP + V_i) state. Symbols are as before.

The ADP strong-binding state represents an another functional state in muscle activity, that altered also significantly compared to rigor and is represented by the following melting temperatures: in *intact healthy muscle* 54, 56.8 and 62.6 °C, for *tendon detached* 54, 55.8 and 62.7 °C as well as for *denervated muscles* 52.5, 56 and 63 °C, respectively.

The largest change in the melting temperatures was observed in the R + ADP + V_i samples (Fig. 7) that are the so-called weak-binding state. The first melting has been changed significantly (53.1 °C) only in case of *denervated muscle* (52.6 °C for intact and 52.3 for tendon detached), but the second one in all affected muscle altered significantly (*intact*: 57.6; *tendon detached*: 56.7 and *denervated*: 56.1 °C). The highest temperature transition was shifted from 70.5 °C (*intact*) to T_{m3} = 62.5 °C (*tendon detached*) and 63.3 °C (*nerve cut*), respectively. This suggests that the shift of melting temperatures is related to significant conformational changes of myosin heads caused by the surgical intervention (see Table 1).

4. Discussion

The DSC scan of intact muscle as reference showed an unfolding at 52.2 °C that disrupted very likely the interchain

Table 1
Thermal parameters of denaturation of muscle fibres in case of different ATP hydrolysis state

	T_{m1} (°C)	T_{m2}(°C)	T_{m3}(°C)	ΔH (Jg^{-1})
Intact	*R*: 52.2 ± 0.2	59.2 ± 0.2	67.8 ± 0.2	2.4 ± 0.1
	R + ADP: 54.0 ± 0.2	56.8 ± 0.2	62.6 ± 0.2	2.3 ± 0.1
	R + ADP + V_i: 52.6 ± 0.2	57.6 ± 0.2	70.5 ± 0.2	2.2 ± 0.1
Tendon detached	*R*: 53.5 ± 0.2	56.8 ± 0.2	61.6 ± 0.2	2.2 ± 0.1
	R + ADP:54 ± 0.3	55.8 ± 0.2	62.7 ± 0.2	2.1 ± 0.1
	R + ADP + V_i: 52.3 ± 0.2	56.7 ± 0.2	62.5 ± 0.2	2 ± 0.1
Denervated	*R*: 52 ± 0.2	56.8 ± 0.2	62.6 ± 0.2	1.9 ± 0.1
	R + ADP:52.5 ± 0.15	56 ± 0.2	63 ± 0.2	2.4 ± 0.2
	R + ADP + V_i: 53.1 ± 0.2	56.1 ± 0.2	63.3 ± 0.2	2.3 ± 0.1

T_ms are melting temperatures and ΔH stands for calorimetric enthalpy (data in average ± S.D.).

interactions referred to the large rod portion of myosin, because this transition temperature was almost independent of presence or absence of nucleotides (see Figs. 6 and 7). Similarly in isolated myosin, the lowest transition temperature was assigned to the tail portions of myosin [28]. The transition T_{m2} = 59.2 °C (Fig. 5) can be attributed to the unfolding of the rest of myosin [25], involving subfragment-2 with considerably higher T_m value [29]. The highest transition temperature (T_{m3} = 67.8 °C, Fig. 5), which seems to be the most sensitive to nucleotide binding, may relate to the motor region of myosin and partly assigned to actin. The fourth transition at about 63 °C, which was derived only by deconvolution, belongs to the melting of the thin filament system. Its existence is more pronounced in Fig. 7, where the overlap between the peaks is more resolved. From other experiments DSC and EPR data showed that the melting point for F-actin filaments was about in the range of 63–67 °C [30–32].

In case of *tendon detached* muscles the fatty infiltration (CT and MRI) and muscle atrophy (reduction in diameter of the muscle fibres revealed by histology) appeared as a functional consequence in the thermal denaturation, as a significant decrease of second and third melting temperatures in ADP and weak-binding states compared with rigor. It should mean that this intervention highly influenced the motor domain of myosin.

The *nerve cut* significantly shifted in rigor T_{m2} and T_{m3} to lower temperature (56.8 and about 62.6 °C) compared with the intact control (Fig. 5), indicating the loosening of fibre structure as a consequence of atrophy (CT and MRI), and increasing number of connective tissues (histology). In case of ADP strong-binding as well as weak-binding T_{m2} and T_{m3} were shifted towards lower values (see Table 1), which might be the sign of a reduced interdomain interaction as a consequence of structure loosening by fatty infiltration (Figs. 6 and 7). It seems this has influence on the interaction of the catalytic domain with the other structural domains of myosin and the actin component became more overlapped indicating the alteration of the motor domain too.

To sum up we can say that the structure and function are inseparable in case of proteins. We have found no previous studies about the thermal changes of fatty infiltration caused by rotator cuff tear and muscle atrophy caused by suprascapular denervation in the literature. The structural data clearly indicated the well-defined and localized alterations in the muscle fiber. DSC was able to follow their functional (biochemical) consequences through the thermal denaturation, because the unfolding of intermediate states of ATP hydrolysis cycle altered significantly: it means that in the surgically evoked states the muscle fibre function differs from the healthy one. This way we have made a further successful step in the line of the application of thermal analysis for medical problem [33–35].

Acknowledgement

SETARAM Micro DSC-II used in experiments was purchased by CO-272 (OTKA).

References

[1] D. Goutallier, J.M. Postel, J. Bergeneau, L. Lavau, M.C. Voisin, Clin. Orthop. 304 (1994) 78.
[2] K. Nakagaki, J. Ozaki, Y. Tomita, S. Tarnai, J. Shoulder Elbow Surg. 3 (2) (1994) 88.
[3] H. Thomazeau, Y. Rolland, C. Lucas, J.M. Duval, F. Langlais, Acta Orthop. Scand. 67 (3) (1996) 264.
[4] J.M. Postel, D. Goutallier, L. Lavau, J. Bergeneau, M.C. Voisin, in: D.F. Gazielly, P. Gleyze, T. Thomas (Eds.), The Cuff, Elsevier, Paris, 1997, pp. 378–383.
[5] J.M. Björkenheim, Acta Orthop. Scand. 60 (4) (1989) 461.
[6] K. Nakagaki, J. Ozaki, Y. Tomita, S. Tarnai, J. Shoulder Elbow Surg. 5 (3) (1996) 194.
[7] J. Phoenix, D. Betal, N. Roberts, T.R. Helliwell, R.H.T. Edwards, Muscle Nerve 19 (3) (1996) 302.
[8] J. Fabis, P. Kordek, A. Bogucki, M. Synder, H. Kolczynska, Acta Orthop. Scand. 69 (6) (1998) 570.
[9] J. Fabis, P. Kordek, A. Bogucki, J. Mazanowska-Gajdowicz, J. Shoulder Elbow Surg. 9 (3) (2000) 211.
[10] J. Fabis, M. Danilewicz, A. Omulecka, Acta Orthop. Scand. 72 (3) (2001) 282.
[11] C. Gerber, B. Fuchs, J. Hodler, J. Bone Joint Surg. 81A (1999) 505.
[12] C. Gerber, A.G. Schneeberger, S.M. Perren, R.W. Nyffeler, J. Bone Joint Surg. 81A (1999) 1281.
[13] H.K. Uhthoff, F. Matsumoto, G. Trudel, K. Himori, J. Orthop. Res. 21 (3) (2003) 386.
[14] P.L. Privalov, S.A. Potekhin, Methods Enzymol. 131 (1986) 4.
[15] M. Zolkiewski, M.J. Redowicz, E.D. Korn, A. Ginsburg, Biophys. Chem. 59 (1996) 365.
[16] A. Bertazzon, T.Y. Tsong, Biochemistry 29 (1990) 6447.
[17] A. Bertazzon, T.Y. Tsong, Biochemistry 29 (1990) 6453.
[18] M.A. Ponomarev, M. Furch, D.I. Levitsky, D.J. Manstein, Biochemistry 39 (2000) 4527.

[19] I. Gazsó, J. Kránicz, Á. Bellyei, D. Lőrinczy, Thermochim. Acta 402 (2003) 117.
[20] D. Lőrinczy, J. Belágyi, Eur. J. Biochem. 268 (2001) 5970.
[21] M. Kiss, J. Belágyi, D. Lőrinczy, J. Therm. Anal. Calorim. 72 (2003) 565.
[22] D. Lőrinczy, M. Kiss, J. Belágyi, J. Therm. Anal. Calorim. 72 (2003) 573.
[23] C.C. Goodno, Proc. Natl. Acad. Sci. U.S.A. 76 (1979) 2620.
[24] C. Wells, C.R. Bagshaw, J. Muscle Res. Cell Motil. 5 (1984) 97.
[25] D. Lőrinczy, J. Belágyi, Biochem. Biophys. Res. Commun. 217 (2) (1995) 592.
[26] D. Lőrinczy, J. Belágyi, Thermochim. Acta 296 (1997) 161.
[27] D. Lőrinczy, N. Hartvig, J. Belágyi, J. Therm. Anal. Calorim. 64 (2001) 651.
[28] K. Samejima, M. Ishioroshi, T. Yashui, Agric. Biol. Chem. 47 (1983) 2373.
[29] C.C. Goodno, T.A. Harris, C.A. Swenson, Biochemistry 15 (1976) 5157.
[30] J. Belágyi, W. Damerau, G. Pallai, Acta Biochim. Biophys. 13 (1978) 85.
[31] A. Bertazzon, G.H. Tian, A. Lamblin, T.Y. Tsong, Biochemistry 29 (1990) 291.
[32] D. Lőrinczy, F. Könczöl, B. Gaszner, J. Belagyi, Thermochim. Acta 322 (1998) 95.
[33] P. Than, Cs. Vermes, B. Schäffer, D. Lőrinczy, Thermochim. Acta 346 (2000) 147.
[34] P. Than, D. Lőrinczy, Thermochim Acta 404 (2003) 149.
[35] Z. Szántó, L. Benkő, B. Gasz, G. Jancsó, E. Rőth, D. Lőrinczy, Thermochim. Acta 417 (2004) 171.